Synthesis and Reactivity of Ferrocenyl functionalized Sn/S Cages

Christopher Pöhlker, Inga Schellenberg, Rainer Pöttgen, Stefanie Dehnen

Fachbereich Chemie, Philipps-Universität Marburg
Hans-Meerwein-Strasse, D-35043 Marburg, Germany

SUPPORTING INFORMATION

(Supplementary Material (ESI) for Chemical Communication)

Experimental Syntheses Details

General: All synthesis steps were performed with strong exclusion of air and external moisture (Ar atmosphere at a high-vacuum, double-manifold Schlenk line or Ar atmosphere in a glove box). All solvents were dried and freshly distilled prior to use. Water was degassed by applying dynamic vacuum (10^{-3} mbar) for several hours.

Synthesis of FcSn(nBu)$_3$: 15.08 g (0.081 mol, 1 eq) of ferrocene were dissolved in 70 mL THF. 47.7 mL *t*BuLi (1.7 M, 1 eq) were added dropwise at r.t. during 30 min. After stirring for further 10 min. the temperature was decreased to –5 °C and 26.38 g (nBu)$_3$SnCl (0.081 mol, 1 eq) in 25 ml THF were added within 60 min. The temperature was raised to r.t. and the reaction mixture was stirred for 25 h. After evaporation of the solvent *in vacuo* residual ferrocene was removed by vacuum sublimation at about 150 °C. FcSn(nBu)$_3$ was obtained as deep red oil by distillation *in vacuo* at 180°C. Yield: 21.93 g (0.046 mol, 57 %). ^{1}H NMR (300 MHz, CDCl$_3$, 25°C): δ = 4.33 (m, 2H, Cp-*H*), 4.10 (s, 5H, Cp-*H*), 4.02 (m, 2H, Cp-*H*), 1.67-1.53 (m, 6H, Alkyl-*H*), 1.40-1.27 (m, 12H, Alkyl-*H*), 1.05-0.90 (m, 9H, Alkyl-*H*); ^{13}C NMR (75 MHz, CDCl$_3$, 25°C): δ = 74.60 (Cp-*C*), 70.44 (Cp-*C*), 68.07 (Cp-*C*), 29.44 (Alkyl-*C*), 27.58 (Alkyl-*C*), 13.87 (Alkyl-*C*), 10.46 (Alkyl-*C*); ^{119}Sn NMR (149 MHz, CDCl$_3$, 25 °C): δ = –18.12; MS (ESI): *m/z* = 476 ([M+H]$^+$); CHN: calculated: C 55.6 %, H 7.7 %, N 0.0 %; found: C 54.2 %, H 8.1 %, N 0.3 %.

Synthesis of FcSnCl$_3$ (1): 6.14 g (0.013 mol, 1 eq) of FcSn(nBu)$_3$ were dissolved in a mixture of 24 ml DCM and 70 ml *n*-hexane. 1.97 ml (4.37 g, 0.017 mol, 1.3 eq) SnCl$_4$ were added dropwise at 0 °C within 10 min. First the reaction mixture was stirred at 0°C for 15 min. and then at 30°C for 10 min. After removal of the solvent *in vacuo*, the obtained mixture of yellow and green solids was dissolved in a mixture of 8.5 ml DCM and 85 ml *n*-hexane. The solution was filtered and the solvent of the resulting clear yellow solution was removed *in vacuo*. The yellow crystalline residue was twice recystallized from hot *n*-hexane and washed twice with cold *n*-hexane. **1** was obtained as a microcrystalline, yellow solid. Yield: 3.24 g (7.93 mmol, 61 %). Single crystals were obtained when the solvent of a solution of **1** in *n*-hexane was slowly evaporated within two weeks. ^{1}H NMR (300 MHz, C$_6$D$_6$-d$_6$, 25 °C): δ = 4.04 (t, 2H, Cp-*H*, $^3J_{HH}$ = 1.26 Hz), 4.00 (s, 5H, Cp-*H*), 3.90 (t, 2H, Cp-*H*, $^3J_{HH}$ = 1.26 Hz); ^{13}C NMR (75 MHz, C$_6$D$_6$-d$_6$, 25 °C): δ = 72.62 (Cp-*C*), 72.51 (Cp-*C*), 70.36(Cp-*C*); ^{119}Sn NMR (149 MHz, C$_6$D$_6$-d$_6$, 25 °C): δ = 359.28; MS (ESI): *m/z* = 410 ([M+H]$^+$); IR (KBr, Nujol): $\tilde{\nu}$ = 1412.1 (m), 1382.8 (m), 1308.2 (m), 1260.7 (s), 1144.3 (m), 1105.8 (s), 1023.8 (s), 816.3 (s), 497.2 (m), 482.5 (m), 365.0 (m), 280.6 (w), 217.5 (w), 182.7 (w), 120.5 (m).

Synthesis of $[Na_6(Me_2CO)_4(OH_2)_6][(FcSn)_3S_6]_2$ (2). 387 mg (0.016 mol, 6 eq) of $Na_2S \cdot 9H_2O$ were dissolved in a mixture of 7 ml H_2O and 6 ml acetone. 440 mg (0.011 mol, 4 eq) of $FcSnCl_3$ (**1**) in 4 ml acetone were added dropwise at –5 °C during 5 min. and the reaction mixture was stirred for further 10 min. After raising the temperature to r.t. the mixture was stirred for 24 h. The solvent is removed slowly within a slight Ar stream. Compound **2** formed a microcrystaline precipitate, which could be isolated by careful decantation. Yield: 807 mg (0.301 mmol, 82 %). Single crystals were obtained by direct layering of an acetone solution with *n*-hexane. ^{1}H NMR (300 MHz, MeOD, 25 °C): $\delta = 4.83$ (s, br, 2H, Cp-*H*), 4.37 (s, br, 2H, Cp-*H*), 4.28 (s, br, 5H, Cp-*H*); ^{13}C NMR (75 MHz, MeOD, 25 °C): $\delta = 74.92$ (Cp), 71.33 (Cp), 69.71(Cp); ^{119}Sn NMR (149 MHz, MeOD, 25 °C): $\delta = 85.34$; MS (ESI): $m/z = 1107$ ($[(Sn_3S_6Fe_3C_{30}H_{30})+H]^+ = [M+H]^+$); IR (KBr, Nujol): $\tilde{\nu} = 3315.8$ (s, br), 2961.0 (s), 2844.5 (m), 1463.2 (m), 1624.0 (m), 1412.1 (m), 1377.1 (m), 1340.6 (m), 1294.2 (m), 1259.9 (w), 1184.4 (m), 1138.6 (m) 1105.1 (m), 1071.8 (m), 1048.8 (m), 1019.2 (s), 1000.8 (m), 960.5 (w), 874.3 (m), 823.6 (m), 667.6 (m), 601.9 (m), 498.0 (s), 486.1 (m), 359.7 (s), 326.9 (m), 259.8 (m), 211.0 (s), 171.0 (s); CHN: calculated C 32.8 %, H 2.6 %, N 0.0 %; found C 27.3 %, H 4.1 %, N 0.03 %.

Synthesis of $[(FcSn)_4S_6]$ (3). To a suspension of 60 mg (0.77 mmol, 6 eq) Na_2S in 10 ml THF 210 mg (0.51 mmol, 4 eq) of $FcSnCl_3$ (**1**) in 10 ml THF were added dropwise at 0°C. The reaction mixture was stirred for 19 h at r.t. and remained unstirred for further 12 h until all precipitate has settled down. After decantation the solvent of the clear orange solution was removed *in vacuo*. Yield: 172 mg (0.122 mmol, 96 %) The obtained orange solid was crystallized by layering a solution in $CHCl_3$ with *n*-pentane. ^{1}H NMR (300 MHz, $CDCl_3$, 25 °C): $\delta = 4.53$ (t, 2H, Cp-*H*, $^3J_{HH} = 1.5$ Hz), 4.42 (s, 2H, Cp-*H*, $^3J_{HH} = 1.5$ Hz), 4.38 (s, 5H, Cp-*H*); ^{13}C NMR (75 MHz, $CDCl_3$, 25 °C): $\delta = 72.75$ (Cp-*C*), 71.58 (Cp-*C*), 69.81 (Cp-*C*); MS (ESI): $m/z = 1407$ ($[M+H]^+$); IR (KBr, Nujol): $\tilde{\nu} = 3084.3$ (s), 2925.4 (s), 2854.8 (s), 1632.6 (m, br), 1462.6 (m), 1409.0 (m), 1377.5 (m), 1303.7 (m), 1191.4 (m), 1139.3 (m), 1105.3 (m), 1056.2 (m), 1020.1 (s), 999.3 (s), 874.8 (m), 860.9 (m), 839.4 (m), 816.3 (s), 732.2 (m), 597.8 (w), 490.7 (s), 478.8 (m), 375.9 (s), 328.3 (m), 269.4 (m), 175.1 (m), 140.9 (m).

Synthesis of $[Na(thf)_{3.5}]_2[(FcSn)_8Ni_3S_{16}] \cdot 2THF$ (4). 20 mg (0.017 mmol, 1 eq) of compound **2**, 9 mg (0.034 mmol, 2 eq) $Ni(acac)_2$ and 18 mg (0.068 mmol, 4 eq) PPh_3 were stirred in 6 ml THF for 20 h at r.t.. Filtration of the resulting deep brown suspension gives a deep red brown and clear solution. Crystals were obtained by direct layering with *n*-hexane. Yield: about 20 mg (0.005 mmol, 50 %).

Details of the X-ray diffraction measurements, structure solutions and refinements

Data of the X-ray structural analyses: T = 100(2) K, MoK_α radiation (λ = 0.71073 Å), graphite monochromator, imaging plate detector system Stoe IPDS 2. All structures were solved by direct methods and refined by full-matrix-least-squares refinement against F^2 using SHELXTL software.[1] H atoms bonded to C atoms were generated assuming idealized geometry and refined using the riding model (U_{eq} set at 1.2U_{eq}(parent atom) for methylene/cyclopentadienyl groups and at 1.5U_{eq}(parent atom) for methyl groups). Displacement ellipsoid diagrams with the labelling scheme and a fragment of the packing of the molecules are provided in figures S2-S7. CCDC reference numbers: CCDC 755030-755032, 755188.

Table S1. Crystallographic and refinement details of **1** and **2** at 100(2) K.

Compound	**1**	**2**
Empirical formula	$C_{10}H_9Cl_3FeSn$	$C_{72}H_{90}O_{10}Fe_6S_{12}Sn_6Na_6$
Formula weight /g·mol^{-1}	410.06	2685.34
Crystal color and shape	thin yellow plates	Yellow rhombouses
Crystal size /mm	0.20x0.15x0.08	0.32x0.28x0.22
Crystal system	monoclinic	triclinic
Space group	$P2_1$/c (No. 13)	P–1 (No. 2)
a/Å	6.8102(5)	12.830(3)
b/Å	9.7587(6)	18.538(4)
c/Å	18.6877(15)	20.011(4)
α/°		79.70(3)
β/°	100.404(6)	81.30(3)
γ/°		81.10(3)
V/Å^3	1220.29(15)	4588.8(17)
Z	4	2
ρ_{calc} /g·cm^{-3}	2.23	1.943
μ(MoK_α) /mm^{-1}	3.85	2.87
Absorption correction type	none (intergrown crystals)	psi-scan
Min / max transmission	–	0.187 / 0.319
2θ range /°	9.18-50.00	2.82-52.00
No. of measured reflections	5375	30816
R(int)	0.0549	0.0357
Indep. refl. / indep. refl. with (I>2σ(I))	2141 / 1248	16699 / 12539
No. of parameters	137	1016
R_1 (I>2σ(I)) / wR_2 (all data)	0.0280 / 0.0768	0.0458 / 0.1116
S (all data)	0.932	0.991
Largest diff. peak / hole /e$^-$·Å^{-3}	0.76 / –0.62	3.03 / –2.02

Table S2. Crystallographic and refinement details of **3** and **4** at 100(2) K.

Compound	**3**	**4**
Empirical formula	$C_{40}H_{36}Fe_4S_6Sn_4$	$C_{116}H_{144}Fe_8Na_2Ni_3O_9S_{16}Sn_8$
Formula weight /g·mol^{-1}	1407.21	3813.70
Crystal color and shape	deep orange rods	black needles
Crystal size /mm	0.19x0.15x0.12	0.45x0.18x0.12
Crystal system	tetragonal	triclinic
Space group	P–42_1c (No. 114)	P–1 (No. 2)
a/Å	13.967(3)	11.989(3)
b/Å	13.967(3)	15.435(3)
c/Å	11.064(2)	20.444(4)
α/°		72.39(3)
β/°		79.23(3)
γ/°		77.20(3)
V/Å^3	2158.3(8)	3486.9(13)
Z	2	1
ρ_{calc} /g·cm^{-3}	2.165	1.816
Flack parameter	0.00(2)	-
μ(MoK$_\alpha$) /mm^{-1}	3.9	2.90
Absorption correction type	psi-scan	psi-scan
Min/max transmission	0.235 / 0.281	0.348 / 0.470
2θ range /°	9.84-53.54	9.46-53.48
No. of measured reflections	8638	32920
R(int)	0.0222	0.0582
Indep. refl. / indep. refl. with ($I>2\sigma(I)$)	2256 / 2228	14586 / 11929
No. of parameters	123	719
R_1 ($I>2\sigma(I)$) / wR_2 (all data)	0.0157 / 0.0431	0.0453 / 0.1275
S (all data)	1.002	1.024
Largest diff. peak / hole /e$^-$·Å^{-3}	0.25 / –0.66	1.96 / -1.09

Compound 1: ($C_{10}H_9Cl_3FeSn$): No structure solution could have been found in the explicit space group $P2_1/m$. A solution was found in $P2_1$ space group and was switched for solution in $P2_1/c$ space group. It was found, that the investigated crystal was pseudomerohedrally twinned. A corresponding twin law (-1 0 0, 0 -1 0, 1 0 1) was found and applied in data reduction, assuming two twinning components (the minor component of about 32% based on refinement with one BASF parameter). This made it possible to provide a fully anisotropic crystal structure model in $P2_1/c$ space group. However, convergence was only achieved when SIMU and DELU restraints were applied for all C atoms.

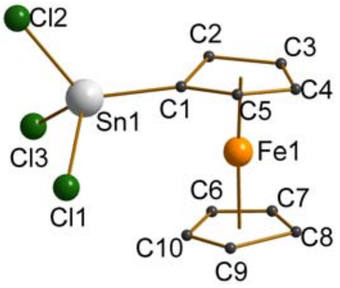

Figure S1. Molecular structure of **1** (H atoms are omitted for clarity). Ball and stick representation is shown for clarity.

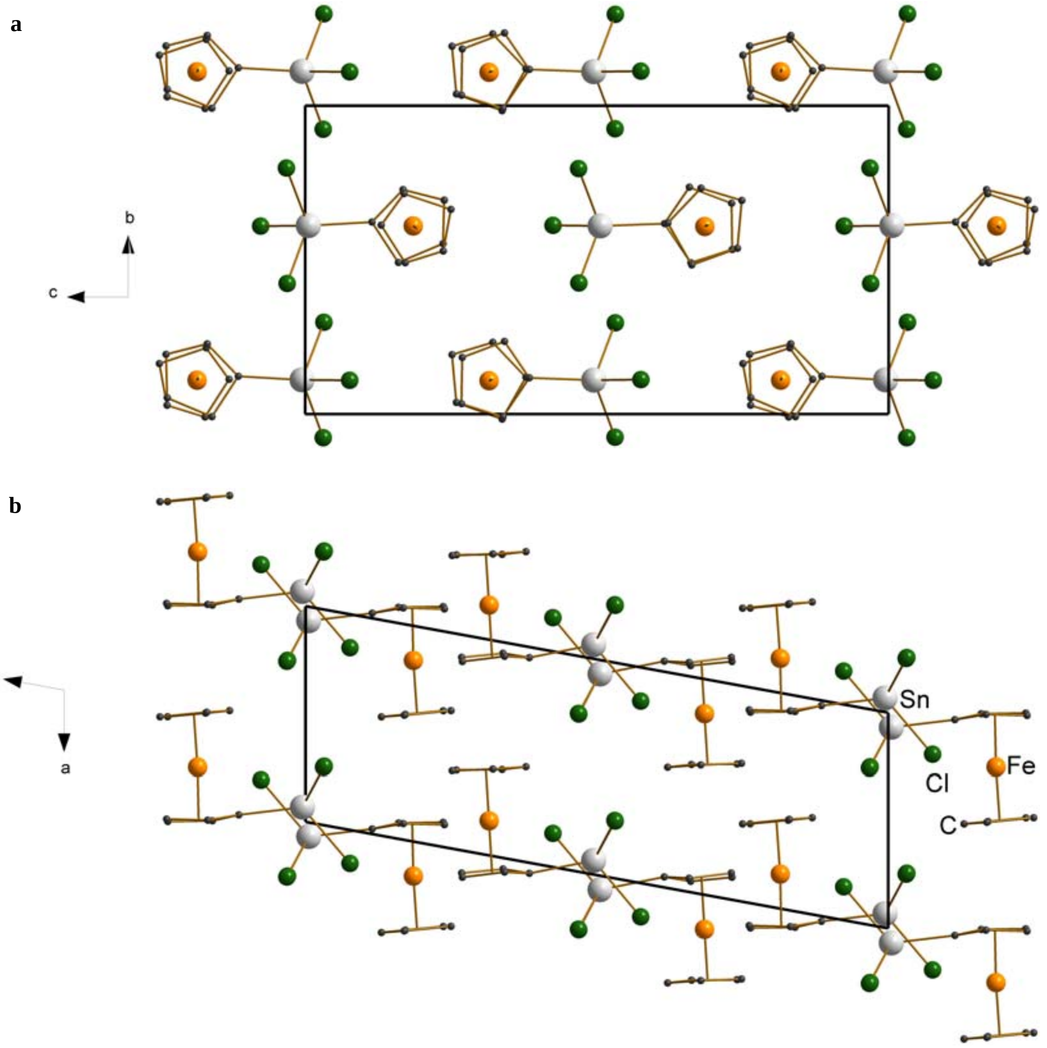

Figure S2. Packing of the molecules of **1** within the crystal, viewed (a) along the crystallographic *a* axis, (b) along the crystallographic *b* axis (H atoms omitted for clarity).

Compound 2: ($C_{72}H_{90}O_{10}Fe_6S_{12}Sn_6Na_6$): Water H atoms could not have been found on difference Fourier map. One acetone molecule (with O1 atom) coordinated to Na1 atom was modelled as disordered in two positions varying in O atom and one methyl C atom positions (major component of 0.56(2) occupancy). SADI restraints were used for the corresponding C-C and C-O bond lengths to keep them at values for one of the ordered acetone molecules. One of the cyclopentadienyl rings in the ferrocene moiety with Fe5 atom was found to be disordered and was modelled assuming two disorder components A and B, consisting of a cyclopentadienyl ring treated as a rigid body (with a corresponding AFIX 59 constraint). Both components were refined anisotropically (major component of occupancy 0.68(3)). Another ferrocene moiety (with Fe2 atom) was found to be severely disordered. It seems, that both cyclopentadienyl rings in this moiety are cooperatively disordered and the Fe2 atom is ordered. A model assuming two disorder components (major component of 0.63(2) occupancy) was proposed; however, it seems that more components should be considered, which may not be performed due to insufficient quality of the available X-ray data. Both components were refined isotropically. In both disordered ferrocene moieties the corresponding C atoms in two components of the disordered cyclopentadienyl rings were restrained using SIMU restraints.

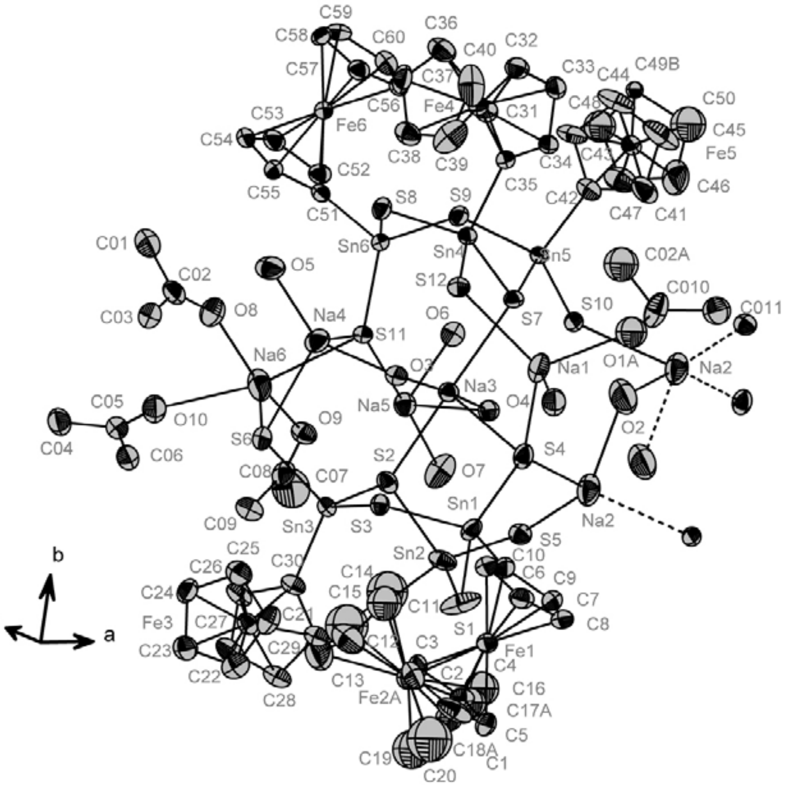

Figure S3. Displacement ellipsoid diagram (50 % probability) of **2**. H atoms and disordered part minor occupancy components are omitted for clarity.

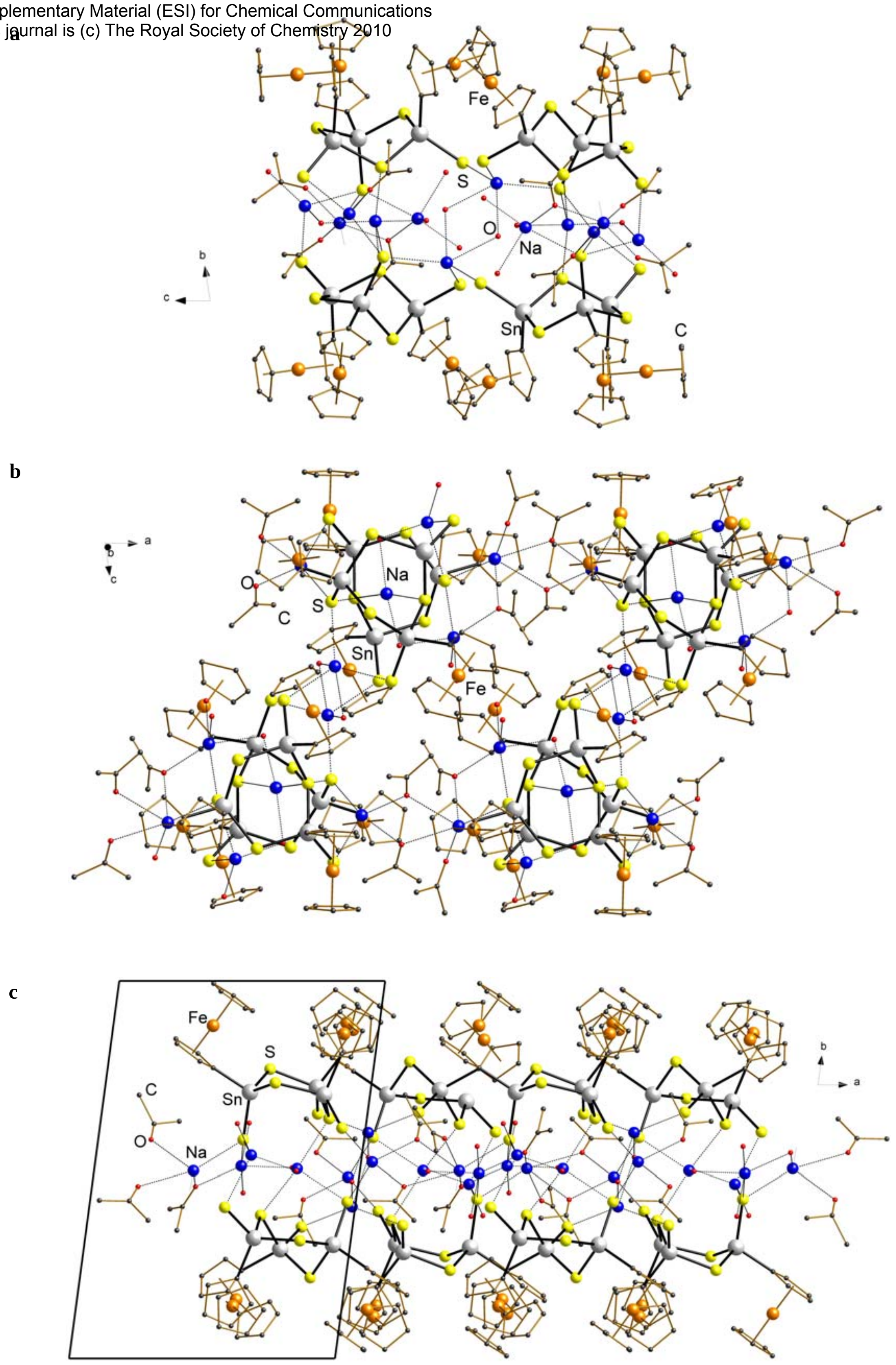

Figure S4. Packing of cations, anions and solvent molecules of **2** within the crystal, viewed (a) along the crystallographic *a* axis, (b) along the crystallographic *b* axis and along the crystallographic *c* axis. H atoms and disordered part minor occupancy components are omitted for clarity.

Compound 3: ($C_{40}H_{36}Fe_4S_6Sn_4$): All non-H atoms refined employing anisotropic displacement parameters. The obtained zero value of Flack parameter confirms the correct assumed absolute configuration.

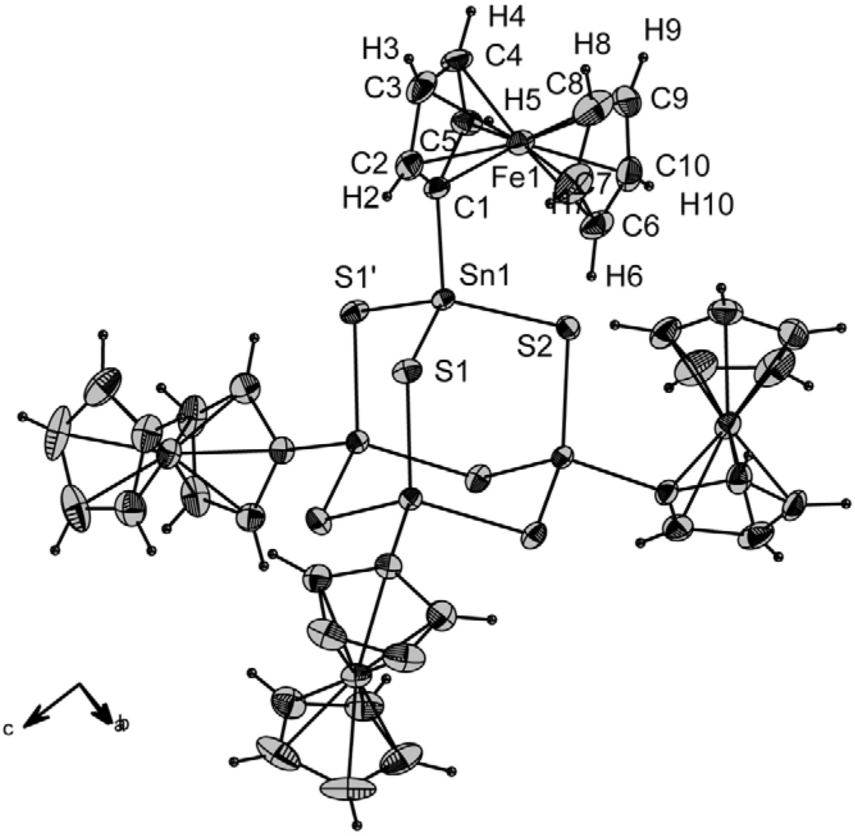

Figure S5. Displacement ellipsoid diagram (50 % probability level) of **3**. Symmetry code ['] y, 1-x, 1-z.

Compound 4: ($C_{116}H_{144}Fe_8Na_2Ni_3O_9S_{16}Sn_8$): In **4** a THF molecule coordinated to Na1 atom occupies an inversion centre, therefore it is disordered in two half-occupied positions (as a consequence, Na1 atom is either 5- or 6-coordinated). Also an alternative structure solution in P1 space group was considered, but it seems, that most plausible model is obtained in $P\bar{1}$ space group. The principle of the THF molecule disorder over an inversion centre is shown in Fig. S8. In the corresponding model EXYZ and EADP constraints were used to keep C53 atoms components (C53A and C53B) on the same site. "PART -1" instruction was used to distinguish between the disordered parts in the crystal structure refinement. All atoms constituting the disordered THF molecule were refined isotropically. Also two other THF molecules (with O1 and O2 atom, respectively; both coordinated to Na1 atom) were found to be disordered in two positions. In case of the molecule with O1 atom, C44 atom was split in two positions (A and B; with major component of 0.65(3) occupancy) and isotropic temperature factors. In case of the molecule with O2 atom two atoms were split into two positions A and B with major component of 0.61(3) occupancy and isotropic temperature factor. The two THF molecules of solvation (with O5A and O6A atoms) are also disordered and the optimal model assumes for them half-occupancy factors and isotropic temperature factors. All C-C and C-O bond lengths in disordered THF molecules (except for the disorder over inversion centre) were restrained by means of SADI restraints to adopt similar values as in case of the ordered THF molecules. For all atoms constituting the disordered THF molecules SIMU and DELU restraints were applied.

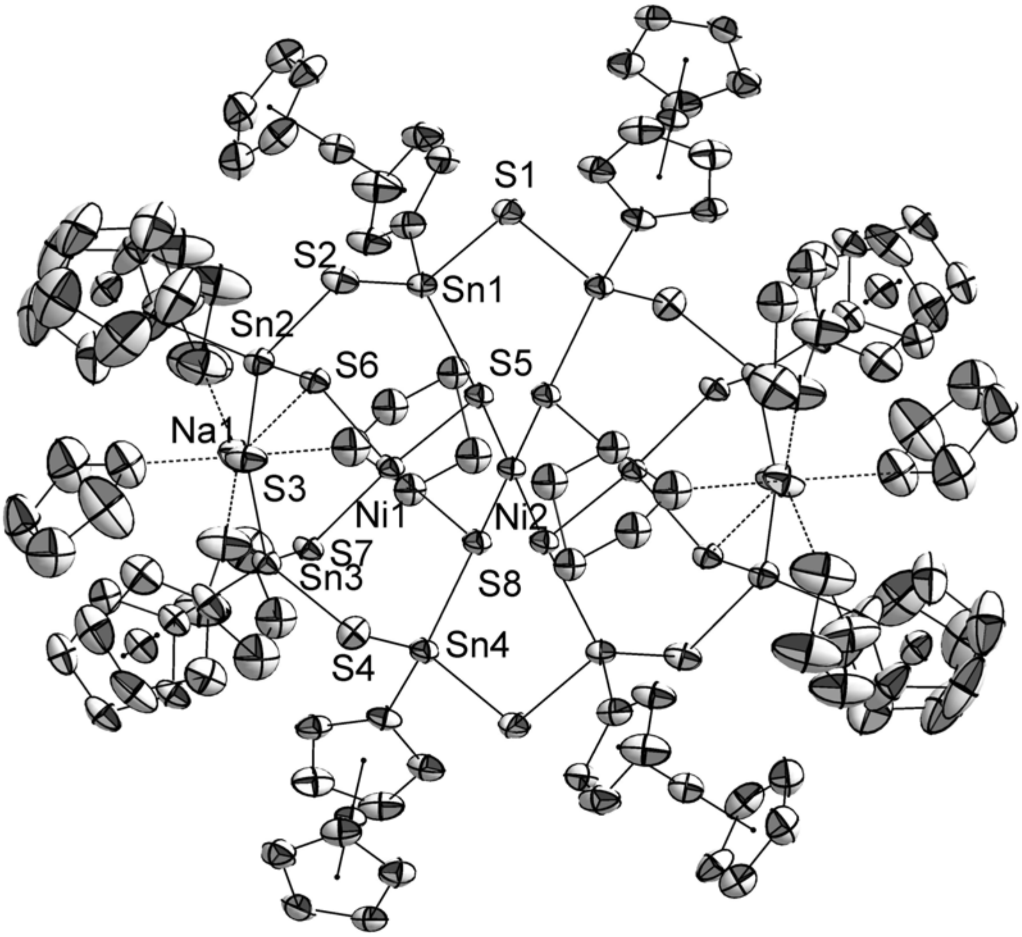

Figure S6. Displacement ellipsoid diagram (50% probability) of **4**. H atoms and disordered part minor occupancy components are omitted for clarity.

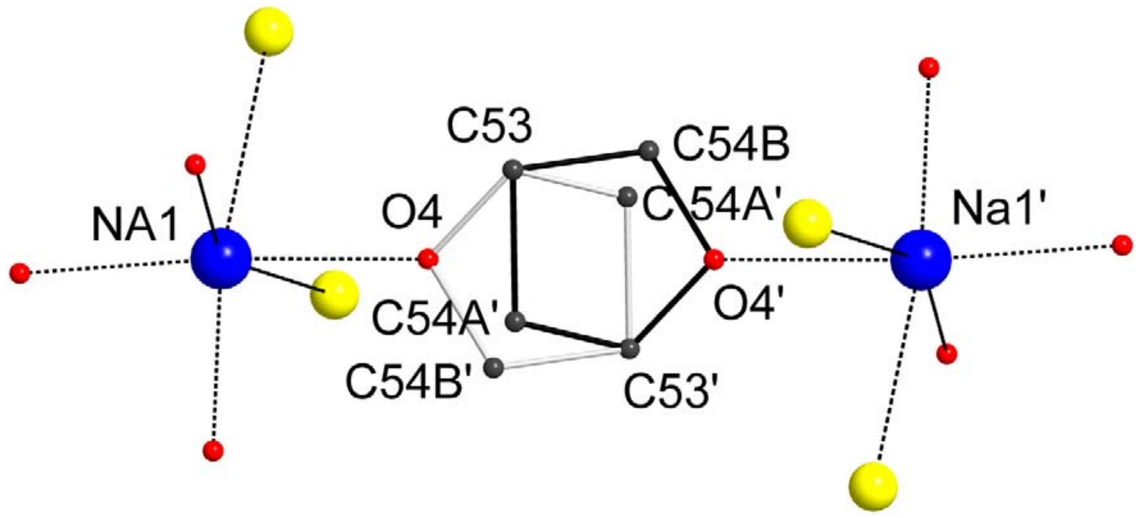

Figure S7. Illustration of the disorder of one coordinating THF molecule which is positioned between two adjacent Na$^+$ ions in **4**. Symmetry code ['] 1-x, 1-y, 1-z.

Table S3. Selected interatomic distances [Å] and angles [°] observed in compounds **1**, **2**, **3** and **4**.

Compound 1			
Fe1–C1	2.046(6)	Sn1–C1	2.060(5)
Fe1–C2	2.080(16)	Sn1–Cl1	2.324(5)
Fe1–C3	2.077(15)	Sn1–Cl2	2.3243(13)
Fe1–C4	2.020(16)	Sn1–Cl3	2.305(4)
Fe1–C5	2.008(15)	Cl1–Sn1–Cl2	103.15 (18)
Fe1–C6	2.050(6)	Cl2–Sn1–Cl3	103.47(17)
Fe1–C7	2.091(17)	C1–Sn1–Cl1	110.8(5)
Fe1–C8	2.067(15)	C1–Sn1–Cl2	120.23(18)
Fe1–C9	2.037(15)	C1–Sn1–Cl3	114.0(5)
Fe1–C10	1.999(17)		

Compound 2			
Sn1–(μ-S1)	2.451(3)	Na3–S7	2.834(3)
Sn1–(μ-S3)	2.4315(17)	Na3–S11	2.918(3)
Sn2–(μ-S1)	2.372(2)	Na4–S6	2.794(4)
Sn2–(μ-S2)	2.419(2)	Na4–S11	2.783(3)
Sn3–(μ-S2)	2.4103(17)	Na5–S2	3.115(3)
Sn3–(μ-S3)	2.4391(17)	Na5–S11	2.799(3)
Sn4–(μ-S7)	2.4286(17)	Na6–S6	3.005(5)
Sn4–(μ-S8)	2.4304(18)	Na6–S11	2.867(4)
Sn5–(μ-S7)	2.4267(18)		
Sn5–(μ-S9)	2.4206(18)	Na1–O10^i	2.443(6)
Sn6–(μ-S8)	2.4176(18)	Na2–O2	2.471(9)
Sn6–(μ-S9)	2.4151(17)	Na3–O3	2.444(5)
Sn1–S$_t$4	2.332(2)	Na3–O4	2.352(5)
Sn2–S$_t$5	2.3254(18)	Na4–O3	2.313(5)
Sn3–S$_t$6	2.328(2)	Na4–O5	2.259(6)
Sn4–S$_t$12	2.3295(18)	Na5–O4	2.426(5)

Sn5–S$_t$10	2.3226(17)	Na5–O6	2.404(5)
Sn6–S$_t$11	2.3303(17)	Na5–O7	2.273(6)
		Na5–O9	2.590(6)
Sn1–C6	2.125(7)	Na6–O8	2.216(7)
Sn3–C30	2.118(7)	Na6–O9	2.316(6)
Sn4–C35	2.110(6)	Na6–O10	2.796(6)
Sn5–C42	2.102(7)		
Sn6–C51	2.118(6)	(μ-S1)–Sn1–(μ-S3)	105.66(8)
Fe1–C1	2.043(8)	(μ-S1)–Sn2–(μ-S2)	106.43(7)
Fe1–C2	2.039(7)	(μ-S2)–Sn3–(μ-S3)	106.86(6)
Fe1–C3	2.030(7)	S$_t$4–Sn1–(μ-S1)	116.05(8)
Fe1–C4	2.045(7)	S$_t$4–Sn1–(μ-S3)	113.35(7)
Fe1–C5	2.040(8)	S$_t$5–Sn2–(μ-S1)	114.19(9)
Fe1–C6	2.032(7)	S$_t$5–Sn2–(μ-S2)	110.08(6)
Fe1–C7	2.031(7)	S$_t$6–Sn3–(μ-S2)	103.48(7)
Fe1–C8	2.035(7)	S$_t$6–Sn3–(μ-S3)	110.72(7)
Fe1–C9	2.024(7)	(μ-S7)–Sn4–(μ-S8)	109.98(6)
Fe1–C10	2.019(7)	(μ-S7)–Sn5–(μ-S9)	109.39(6)
Na1–S4	2.830(4)	(μ-S8)–Sn6–(μ-S9)	113.36(6)
Na1–S12	2.858(4)	S$_t$10–Sn5–(μ-S7)	106.53(6)
Na2–S4	2.851(4)	S$_t$10–Sn5–(μ-S9)	109.60(7)
Na2–S5	2.781(4)	S$_t$11–Sn6–(μ-S8)	110.17(7)
Na2^{i}–S10	2.821(4)	S$_t$11–Sn6–(μ-S9)	114.30(6)
Na3–S2	2.859(3)	S$_t$12–Sn4–(μ-S7)	101.19(6)
Na3–S4	2.866(3)	S$_t$12–Sn4–(μ-S8)	114.40(6)

Symmetry codes: (i) −x+2, −y+1, −z; (ii) x+1, y, z.

Compound 3

Sn1–S1	2.3894(8)	Fe1–C8	2.045(3)
Sn1–S2	2.4009(7)	Fe1–C9	2.033(3)
Sn1–C1	2.095(3)	Fe1–C10	2.052(3)
Fe1–C1	2.039(3)		
Fe1–C2	2.032(3)	S1–Sn1–S2	112.61(2)
Fe1–C3	2.042(3)	Sn1–S1–Sn1^{i}	104.77(3)
Fe1–C4	2.055(3)	Sn1–S2–Sn1^{ii}	104.28(4)
Fe1–C5	2.046(3)	C1–Sn1–S1	103.85(9)
Fe1–C6	2.061(3)	C1–Sn1–S2	110.32(8)
Fe1–C7	2.044(3)		

Symmetry codes: (i) −y+1, x, −z+1; (ii) −x+1, −y+1, z.

Compound 4

Sn1–(μ-S1)^{i}	2.4279(16)	Fe2–C9	2.048(6)
Sn1–(μ-S2)	2.4274(15)	Fe2–C10	2.045(6)
Sn2–(μ-S2)	2.3913(15)		
Sn2–(μ-S3)	2.3932(17)	(μ-S1)^{i}–Sn1–(μ-S2)	94.52(6)
Sn3–(μ-S3)	2.4026(14)	(μ-S2)–Sn2–(μ-S3)	109.90(6)
Sn3–(μ-S4)	2.3953(16)	(μ-S3)–Sn3–(μ-S4)	110.31(6)
Sn4–(μ-S4)	2.3974(14)	(μ-S4)–Sn4–(μ-S1)	101.72(6)
Sn4–(μ-S1)	2.4063(18)	(μ-S1)^{i}–Sn1–S$_t$5	107.09(5)
Sn1–S$_t$5	2.4413(14)	(μ-S2)–Sn1–S$_t$5	118.76(5)
Sn2–S$_t$6	2.3725(13)	(μ-S2)–Sn2–S$_t$6	98.27(5)
Sn3–S$_t$7	2.3610(13)	(μ-S3)–Sn2–S$_t$6	118.14(5)

Sn4–S$_t$8	2.4371(15)	(μ-S3)–Sn3–S$_t$7	117.48(5)
Sn1–C1	2.128(5)	(μ-S4)–Sn3–S$_t$7	103.85(5)
Sn2–C11	2.129(6)	(μ-S4)–Sn4–S$_t$8	111.11(5)
Sn3–C21	2.107(5)	(μ-S1)–Sn4–S$_t$8	108.47(6)
Sn4–C31	2.127(5)	Sn1–(μ-S2)–Sn2	95.98(5)
Ni1–Ni2	2.9679(12)	Sn2–(μ-S3)–Sn3	107.20(5)
Ni1–S$_t$5	2.2025(15)	Sn3–(μ-S4)–Sn4	96.50(5)
Ni1–S$_t$6	2.2336(16)	Sn4–(μ-S1)–Sn1^i	107.69(6)
Ni1–S$_t$7	2.2348(14)	S$_t$5–Ni1–S$_t$6	93.01(6)
Ni1–S$_t$8	2.2106(16)	S$_t$6–Ni1–S$_t$7	92.33(6)
Ni2–S$_t$5	2.2134(15)	S$_t$7–Ni1–S$_t$8	95.25(5)
Ni2–S$_t$8	2.2259(13)	S$_t$8–Ni1–S$_t$5	79.25(5)
Na1–S$_t$6	2.854(3)	S$_t$5–Ni2–S$_t$8	78.69(5)
Na1–S$_t$7	3.018(3)	S$_t$5^i–Ni2–S$_t$8	101.31(5)
Fe2–C1	2.034(6)	Ni1–Ni2–Ni1^i	180.0
Fe2–C2	2.043(6)	S$_t$5–Sn1–C1	110.62(15)
Fe2–C3	2.048(6)	S$_t$6–Sn2–C11	116.82(16)
Fe2–C4	2.047(6)	S$_t$7–Sn3–C21	116.81(13)
Fe2–C5	2.028(6)	S$_t$8–Sn4–C31	117.42(13)
Fe2–C6	2.039(6)		
Fe2–C7	2.029(6)		
Fe2–C8	2.033(7)		

Symmetry codes: (i) −x+2, −y+1, −z+1.

Mössbauer spectroscopy

A Ca^{119m}SnO$_3$ source was available for the ^{119}Sn investigation and a palladium foil of 0.05 mm thickness was used to reduce the tin K X-ray concurrently emitted by this source. A ^{57}Co/Rh source was used for the ^{57}Fe Mössbauer spectroscopic investigations. The measurements were performed in the usual transmission geometry in commercial helium bath and flow cryostats. The temperature of the absorber could be varied from 4.2 to 300 K. The sources were kept at room temperature in all experiments. The samples were placed in sealed glass containers at a thickness corresponding to about 10 mg of the Mössbauer active element/cm^2. Figures S8 and S9 show the ^{119}Sn and ^{57}Fe Mössbauer spectra of **2** and **3** at 4.2 K and 77 K.

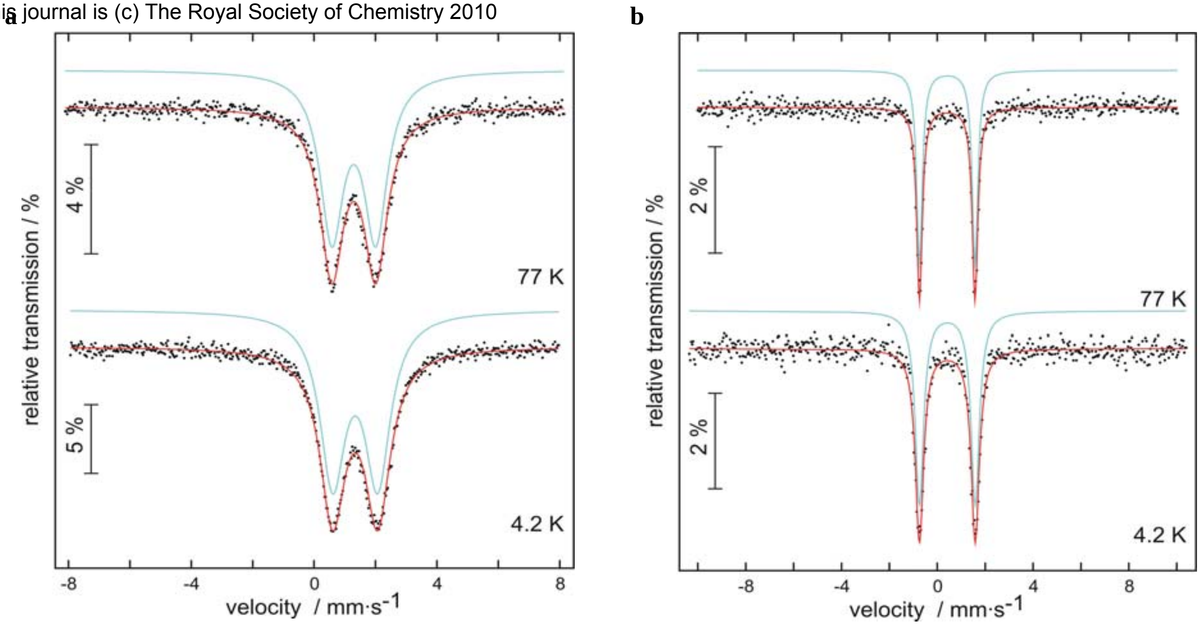

Figure S8. Mössbauer spectra of **2** at 4.2 K and 77 K. (a) ^{119}Sn, (b) ^{57}Fe. The red lines represent fit curves for Sn^{IV} (a) Fe^{II} (b).

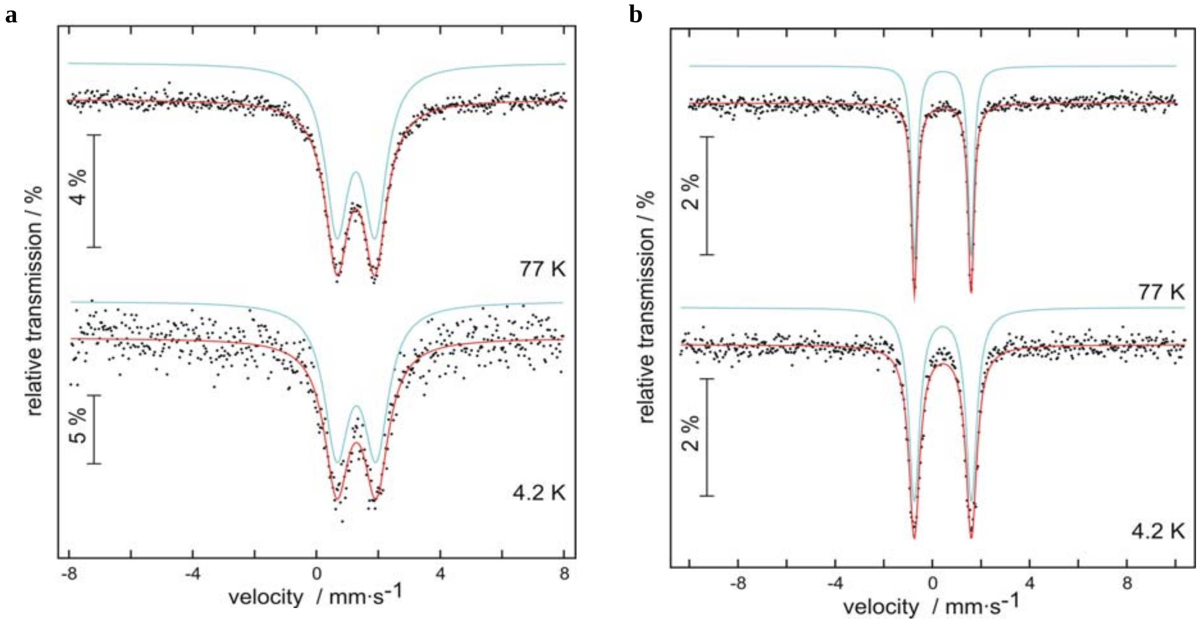

Figure S9. Mössbauer spectra of **3** at 4.2 K and 77 K. (a) ^{119}Sn, (b) ^{57}Fe. The red lines represent fit curves for Sn^{IV} (a) Fe^{II} (b).

Quantum chemical investigations

DFT[2] investigations of the anion in **2** were undertaken using the program system TURBOMOLE[3] (RIDFT program,[4] Becke-Perdew 86 (BP86) functional,[5] gridsize m3). Basis sets were of def2-TZVP quality (TZVP = triple zeta valence plus polarization).[6] For Sn atoms an effective core potential (ECP-28)[7] has been used for consideration of relativistic corrections and to reduce the computational effort. The high negative charge was compensated for by employment of the COSMO model.[8]

Figure S10 illustrates the different conformers of the anion in **2** and indicates relative energies with respect to the global minimum structure Twist* (= resulting structure when simultaneously optimizing electronic and geometric structure of the boat-type conformer). Figure S11 shows the course of the energy during this optimization, starting out from the experimentally observed, boat-type conformer.

Twist*: ±0 kJ·mol^{-1} (see below)

Twist: +4.8 kJ·mol^{-1}

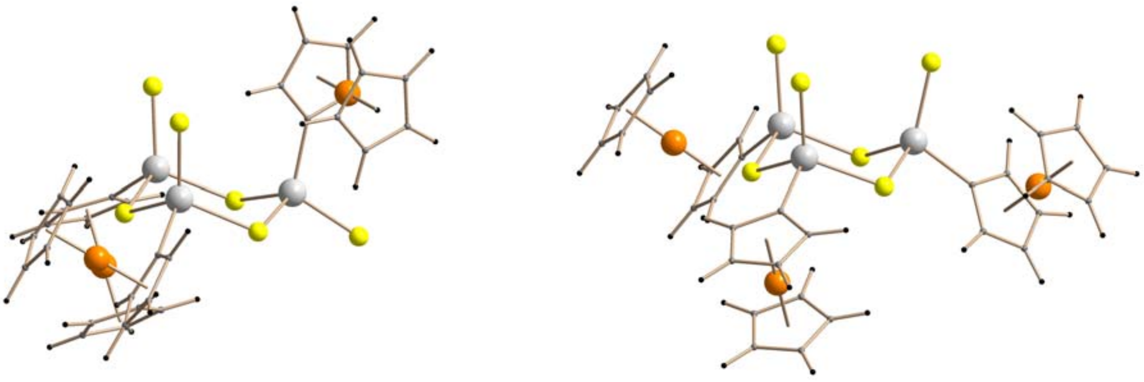

Chair_anti: +12.5 kJ·mol^{-1}

Chair_syn: ±16.3 kJ·mol^{-1}

Figure S10. DFT-optimized structural isomers of the anion in **2** together with relative energies with respect to the most stable one. Twist* denotes the structure resulting upon simultaneous optimization of electronic and geometric structure of the experimentally observed, boat-type conformer. Anti and Syn denote different orientations of the terminal S ligands with respect to the Sn_3S_3 six-membered ring in the chair-typeconformation of the truncated adamantane-type structure.

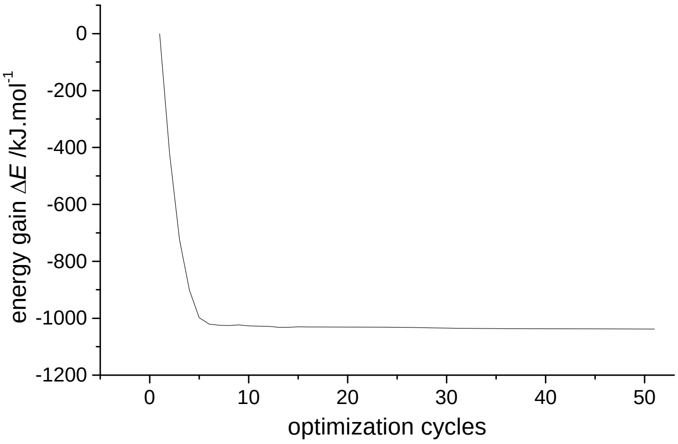

Figure S11. Course of the energy during the rearrangement of the Boat structure (X-Ray structural data) to the Twist* structure, which occurs during the simultaneous optimization of geometric and electronic structure (given as energy gain from an arbitrary starting value of 0).

References for supporting information

[1] G. M. Sheldrick, SHELXTL 5.1, Bruker AXS Inc., 6300 Enterprise Lane, Madison, WI 53719–1173, USA, **1997**.

[2] a) R. G. Parr, W. Yang, *Density Functional Theory of Atoms and Molecules*, Oxford University Press, New York **1988**; b) T. Ziegler, *Chem. Rev.* **1991**, *91*, 651–667.

[3] a) R. Ahlrichs, M. Bär, M. Häser, H. Horn, C. Kölmel, *Chem. Phys. Lett.* **1989**, *162*, 165–169; b) O. Treutler, R. Ahlrichs, *J. Chem. Phys.* **1995**, *102*, 346–354.

[4] a) K. Eichkorn, O. Treutler, H. Öhm, M. Häser, R. Ahlrichs, *Chem. Phys. Lett.* **1995**, *242*, 652–660; b) K. Eichkorn, F. Weigend, O. Treutler, R. Ahlrichs, *Theor. Chim. Acta* **1997**, *97*, 119–124.

[5] a) A. D. Becke, *Phys. Rev. A* **1988**, *38*, 3098–3109; b) S. H. Vosko, L. Wilk, M. Nusair, *Can. J. Phys.* **1980**, *58*, 1200–1205; c) J. P. Perdew, *Phys. Rev. B* **1986**, *33*, 8822–8837.

[6] F. Weigend, R. Ahlrichs, *Phys. Chem. Chem. Phys.* **2005**, *7*, 3297–3305.

[7] B. Metz, H. Stoll, M. Dolg, *J. Chem. Phys.* **2000**, *113*, 2563.

[8] a) A. Klamt, G. Schürmann, *J. Chem. Soc. Perkin Trans.* **1993**, *5*, 799–805; b) A. Schäfer, A. Klamt, D. Sattel, J. C. W. Lohrenz, F. Eckert, *Phys. Chem. Chem. Phys.* **2000**, *2*, 2187–2193.